Robotics and Autonomous Systems 114 (2019) 19–28

Contents lists available at ScienceDirect

Robotics and Autonomous Systems

journal homepage: www.elsevier.com/locate/robot

Stiffness feasible workspace of cable-driven parallel robots with application to optimal design of a planar cable robot

Javad Bolboli, Mohammad A. Khosravi *, Farzaneh Abdollahi

The Center of Excellence on Control and Robotics, Department of Electrical Engineering, Amirkabir University of Technology (Tehran Polytechnic), Iran

HIGHLIGHTS

- Internal forces may decrease the overall stiffness of the cable robot.
- Based on the above fact, stiffness-feasible workspace is introduced.
- In this workspace increasing the internal forces can modify the total stiffness of the robot.
- Defining some performance criteria.
- Optimal design of the robot based on the proposed criteria.

ARTICLE INFO

Article history:
Received 13 August 2018
Received in revised form 16 December 2018
Accepted 15 January 2019
Available online 22 January 2019

Keywords:
Cable-driven parallel robot
Stiffness
Internal forces
Stiffness-feasible workspace
Optimal design

ABSTRACT

In this paper stiffness of cable-driven parallel robots (CDPRs) is analyzed in detail and based on this analysis, the stiffness-feasible workspace is introduced. This workspace includes all stable poses which increasing the internal forces can modify the total stiffness of the robot. It has been shown that in the CDPRs, the concept of the internal forces can be applied for keeping cables in tension and increasing stiffness. However, it should be noted that increasing the internal forces may decrease the overall stiffness of the mechanism and it is only applicable in stabilizable poses of the workspace. Therefore, stiffness-feasible workspace determines the allowable internal forces range which can increase the stiffness and it will guarantee that in this range of the internal forces, the structure of the robot is stable. In this paper, by employing this criterion and evolutionary algorithms, a CDPR is optimally designed, and a set of answers is presented. In this design, in addition to the stiffness-feasible workspace, another criterion as stiffness number is presented which is useful for specifying the distribution of the stiffness and stiffness-feasibility of the robot.

1. Introduction

Cable-driven parallel robots (CDPRs) are mechanisms with closed kinematic chains which use low weight cables instead of the rigid links. The end-effector of the CDPRs is connected to a fixed frame with cables that reel around winches and winches regulate the pose of the end-effector to the desired position. Owing to low weight links and simple structure, CDPRs have many potential advantages such as high acceleration, large workspace, fast motion, and low-cost [1]. Advantages of CDPRs comparing to the rigid link mechanisms provide great motivations to use these mechanisms in several industrial applications [2], such as movement and lifting heavy loads [3], cable-suspended camera systems [4], grasping [5], radio telescope [6] and space and terrestrial applications [7].

However, the inherent property of the cables that they cannot push and only pull arises several challenges such as keeping cables in tension and low stiffness of the robot. Based on this fact, two different classes of CDPRs are introduced. In completely restrained CDPRs which are studied in this paper, for n degrees of freedom, at least $n + 1$ driving cable must be employed and incompletely restrained CDPRs which employ an external force such as, gravity to keeping cables taut [8,9].

Due to the property of the cables which must be taut, workspace analysis of these mechanisms is accompanied by methods to check the tension of the cables such as, geometry approaches and methods which investigate the null space of the Jacobian transpose [10]. Among the different types of the workspaces of the cable robots, Wrench Closure Workspace(WCW) is defined as a set of poses of the end-effector where robot able to apply any wrench while cables are taut [11,12]. It is shown that any pose X belongs to the WCW if and only if the Jacobian matrix $\boldsymbol{J}$ has full rank and the null space of the Jacobian transpose contains a vector $\boldsymbol{z} > \boldsymbol{0}$ ($\boldsymbol{J}^T\boldsymbol{z} = \boldsymbol{0}$).

* Corresponding author.
E-mail addresses: j.bolboli@aut.ac.ir (J. Bolboli), m.a.khosravi@aut.ac.ir (M.A. Khosravi), f_abdollahi@aut.ac.ir (F. Abdollahi).

https://doi.org/10.1016/j.robot.2019.01.012
0921-8890/

This characterization shows that the WCW depends only on the robot geometry.

Maximizing volume of the workspaces is a valuable criterion in the design of CDPRs. Pusey et al. [13] used this kind of criterion as a cost function for design optimization of a 6 DOF cable robot. In [14] the grouped coordinate descent method is applied and the mechanical structure of a 6-DOF cable-driven parallel robot with eight cables is optimized. The grouped coordinate descent method can guarantee the final design parameter of the robot is symmetric. In [15] a parallel robotic platform in a marine environment is analyzed dynamically in order to find the workspace of four different designs of the robot and changing the cables' layout and environmental loads are introduced as effective factors on the workspace. In [16] the shape and size of the end-effector of CDPR are optimized to maximize the volume of the stable workspace. However, in this research, the adverse effects of the internal forces on the stiffness of the mechanism are not investigated.

In the cable robots, the internal forces are defined as forces in the cables of the mechanism where externally applied wrench is zero. Notice that since the internal force lies in the null space of Jacobian transpose, it does not contribute into the driving force to the end-effector, and it only produces tension in the cables in order to keep all the cables in positive tension. Kawamura et al. [17] have indicated that in completely restrained CDPRs internal forces can play a vital role in reducing the vibration of the end-effector and improving the stiffness. Many studies point out that stiffness is a function of internal forces, the pose of the end-effector and the geometry of the mechanism, which may apply considerable instability and low position accuracy problems [18,19]. In [20] stiffness matrix of CDPRs considering four spring model for the cables has been presented and the root of instability has been analyzed. They have mentioned that the internal forces in these mechanisms create the internal forces stiffness. Here stability means that the end-effector tendency to return to the static equilibrium when robot undergoes an external disturbance. In the most of researches, workspaces are defined by considering the inherent property of the cables that they must be taut in the whole maneuver space of the robot such as WCW and WFW and the main concern of few research is stiffness and the adverse effects of internal forces on the volume of the workspace. It is notable that the overall stiffness of the CDPRs is the summation of two stiffnesses: stiffness of the cables and stiffness of the internal forces. In many mechanisms and studies, the stiffness of the internal forces has ignored. Whereas in some poses of the end-effector, the internal forces stiffness is dominant and not only it does not modify the stiffness of the mechanism, but also it may make the mechanism unstable even in the WCW. These dual properties of the internal forces stiffness lead us to design an appropriate mechanism to improve the total stiffness of the mechanism.

Considering the effects of mechanical structure on the stiffness and other desired characteristics of the robot, many studies on the optimal design of CDPRs have been done. Yeo et al. [18] presented a simple scalar index to quantify the magnitude of the stiffness. Abdolshah et al. [21] studied motions and location of pulley blocks of CDPR as a function of the pose of the end-effector to optimize stiffness and dexterity. In [22] to maximize the ratio of SFW and WCW, mechanical structure and the geometry configurations of the CDPR are optimized. As a mechanical approach to achieve optimal stiffness, a couple of springs are attached to the direction of cables in the cable mobile robot [23]. Yu et al. [24] used actuation redundancy to achieve the desired end-effector stiffness. Jamshidifar et al. [25] in order to achieve optimal stiffness, considered stiffness magnitude of the end-effector as an objective function and then by employing a redundancy resolution, an approach is developed to maximize the objective function. A stiffness optimization approach provided by Mendez et al. [26] to minimize the lowest natural frequencies as an objective function in the design of CDPR for warehousing applications. Moradi et al. studied a CDPR with two DOF and to maximize the area of the stiffness maps, the position of the cable attachment points are identified [27].

To the best of the authors' knowledge, none of the above-mentioned studies has not specified a set of poses of the end-effector as a workspace where the robot could use allowable values of internal forces for modifying the total stiffness of the robot. As it mentioned earlier, in some poses of the robot in the maneuver space, increasing internal forces have a negative impact on the overall stiffness of the mechanism. As a result, a cable robot always endures a concern of unexpected collapse and vibration in the aforementioned workspaces. These facts highlight the necessity of introducing a new workspace based on the effects of internal forces on the stiffness and optimal design of CDPRs. In this paper first, considering the vital role of the internal forces on the total stiffness of the robot Stiffness Feasible Workspace (SFW) is introduced. To define this workspace, the allowable internal forces range which will guarantee the stability of the mechanism is considered. Moreover, Stiffness Number (SN) criterion is presented which indicates the distribution of the stiffness of the structure. Next, the effects of design parameters on the SFW volume and SN are studied. Relying on the essential role of the internal forces in the performance of CDPRs, an optimization method is applied to optimize the design parameters by maximizing the volume of the SFW, WCW, and uniform distribution of the stiffness. However, it is notable that the opposite effects of the design parameters on the proposed criteria lead us to use multi-objective optimization methods. Therefore, for a planar cable robot, an evolutionary algorithm (EA) is implemented to obtain a set of optimal answers. Then, due to the rank of importance of the optimization criteria, the design parameters based on the application and conditions can be selected from the set of answers.

The rest of the paper organized as follows: In Section 2 stiffness analysis of the CDPR is described, in Section 3 stiffness-feasible workspace on CDPRs is defined. Section 4 develops the criteria to the optimal design of CDPRs. Optimization parameters and effects of optimization parameters are discussed in Section 5. In Section 6, the results of the optimization problem are presented and the paper is finally concluded in Section 7.

2. Stiffness

In the CDPRs, deflection of the end-effector caused by the applied wrench under static equilibrium shows the stiffness of the mechanism. In this class of the robots, due to the property of the cables that cannot push and can only pull, redundancy in actuators is essential. Redundancy in actuators creates internal forces whose resultant wrench on the end-effector of the robot is zero, but these forces create internal forces stiffness.

General model of a CDPR with m degree of freedom and n cable is shown in Fig. 1. Assume that $d\mathbf{p}$ and $d\mathbf{l}$ represent the vector of small displacements of the end-effector and cable coordinates, to find the overall stiffness of the mechanism using virtual work principal the static balance equation can be written as:

$$\mathbf{J}^T\boldsymbol{\tau} + \mathbf{F}_o = \mathbf{0} \tag{1}$$

where $\mathbf{F}_o$ is external wrench applied to the end-effector, $\mathbf{J} = \dfrac{d\mathbf{l}}{d\mathbf{p}}$ and $\boldsymbol{\tau}$ are the Jacobian matrix of the robot and the vector of the cable forces, respectively.

Utilizing the derivative of Eq. (1) with respect to the position of the end-effector in task space, stiffness matrix can be written as follow.

$$\mathbf{K} = -\frac{d\mathbf{F}_o}{d\mathbf{p}} = \mathbf{J}^T\frac{d\boldsymbol{\tau}}{d\mathbf{l}}\frac{d\mathbf{l}}{d\mathbf{p}} + \frac{d}{d\mathbf{p}}\mathbf{J}^T\boldsymbol{\tau} \tag{2}$$

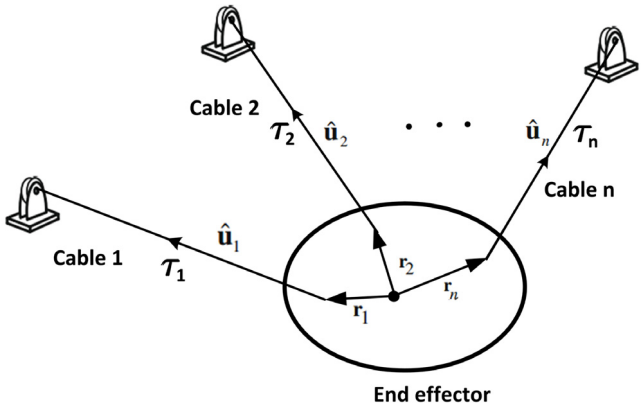

Fig. 1. General model of CDPRs.

in which $\frac{d\mathbf{l}}{d\mathbf{p}}$ is the Jacobian matrix and $\frac{d\boldsymbol{\tau}}{d\mathbf{l}}$ is cable stiffness and hence

$$\mathbf{K} = -\frac{d\mathbf{F}_o}{d\mathbf{p}} = \mathbf{J}^T diag(k_1, k_2, \ldots, k_n)\mathbf{J} + \frac{d}{d\mathbf{p}}\mathbf{J}^T\boldsymbol{\tau} \tag{3}$$

where $k_i s$ are stiffness due to the cables elasticity and actuator stiffness. The second term of the above equation is the stiffness caused by the internal forces. By using four spring model, the effects of the cables elasticity and internal forces on total stiffness of CDPRs can be written as [20]:

$$\mathbf{K} = \mathbf{K}_e + \mathbf{K}_p \tag{4}$$

Where $\mathbf{K}_e$ is due to elasticity in cables and $\mathbf{K}_p$ is due to the internal forces. $\mathbf{K}_e$ and $\mathbf{K}_p$ can be expressed in terms of geometry and cables properties as follows [20]:

$$\mathbf{K}_e = \sum_{i=1}^{n} k_i \begin{bmatrix} \hat{\mathbf{l}}_\mathbf{i}^T & \hat{\mathbf{l}}_\mathbf{i}\hat{\mathbf{l}}_\mathbf{i}^T[\hat{\mathbf{b}}_\mathbf{i}\times]^T \\ [\hat{\mathbf{b}}_\mathbf{i}\times]\hat{\mathbf{l}}_\mathbf{i}\hat{\mathbf{l}}_\mathbf{i}^T & [\hat{\mathbf{b}}_\mathbf{i}\times]\hat{\mathbf{l}}_\mathbf{i}\hat{\mathbf{l}}_\mathbf{i}^T[\hat{\mathbf{b}}_\mathbf{i}\times]^T \end{bmatrix} \tag{5}$$

$$\mathbf{K}_p = \sum_{i=1}^{n} \frac{\tau_i}{l_i} \begin{bmatrix} \mathbf{I} - \hat{\mathbf{l}}_\mathbf{i}\hat{\mathbf{l}}_\mathbf{i}^T & [\hat{\mathbf{b}}_\mathbf{i}\times]^T - \hat{\mathbf{l}}_\mathbf{i}\hat{\mathbf{l}}_\mathbf{i}^T[\hat{\mathbf{b}}_\mathbf{i}\times]^T \\ [\hat{\mathbf{b}}_\mathbf{i}\times] - [\hat{\mathbf{b}}_\mathbf{i}\times]\hat{\mathbf{l}}_\mathbf{i}\hat{\mathbf{l}}_\mathbf{i}^T & [\hat{\mathbf{b}}_\mathbf{i}\times][\hat{\mathbf{b}}_\mathbf{i}\times]^T - [\hat{\mathbf{b}}_\mathbf{i}\times]\hat{\mathbf{l}}_\mathbf{i}\hat{\mathbf{l}}_\mathbf{i}^T[\hat{\mathbf{b}}_\mathbf{i}\times]^T \end{bmatrix} - \sum_{i=1}^{n} \tau_i \begin{bmatrix} \mathbf{0} & \mathbf{0} \\ \mathbf{0} & [\hat{\mathbf{l}}_\mathbf{i}\times][\hat{\mathbf{b}}_\mathbf{i}\times] \end{bmatrix} \tag{6}$$

where $[\hat{\mathbf{l}}_\mathbf{i}\times]$ is the matrix operator of cross product, $\hat{\mathbf{l}}_\mathbf{i}$ is unit vector of ith cable, $\hat{\mathbf{b}}_\mathbf{i}$ is moment arm vector from the center of mass of the end-effector to the attachment point of ith cable and $\mathbf{I}$ is identity matrix. τ_i, l_i and k_i are also coefficients of the internal force, cable length and elastic stiffness, respectively.

According to Eqs. (4), (5) and (6), if τ_i consists of only internal force, sufficient and necessary condition for stabilizability of the robot is positive definiteness of the stiffness matrix $\mathbf{K}$ [20]. It can be shown that the matrix $\mathbf{K}_e$ is symmetric and is always positive definite. The second term of the total stiffness matrix $\mathbf{K}_p$, given in (6) is included of two terms as

$$\mathbf{K}_p = \mathbf{K}_p^a - \mathbf{K}_p^f \tag{7}$$

where due to Eq. (6), $\mathbf{K}_p^a$ is symmetric and is always positive definite. $\mathbf{K}_p^f$ denotes purely rotational stiffness and it is symmetric when all forces are the internal forces. In CDPRs, by increasing the internal forces this part may be larger than the other parts. In that case, the total stiffness matrix is not positive definite and as a result, the robot will be unstable. Regarding this fact, the root of instability is rotational stiffness caused by the internal forces which may even happen in rigid robots [20].

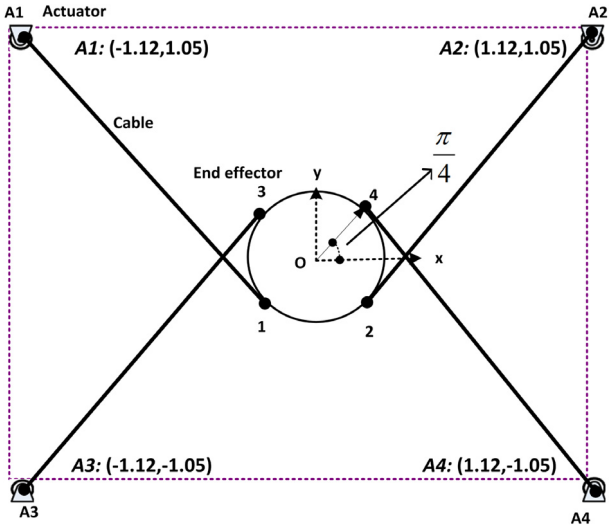

Fig. 2. Dimension and position of attachment points of planar cable-driven parallel robot.

3. Stiffness-feasible workspace

Considering the inherent property of cables that can only pull, cables must be taut in all maneuvers of the robot. This condition has an essential role in robot performance. In [11], Wrench Closure Workspace (WCW) is defined as a set of poses of the end-effector in which for any external wrench exerted onto the moving-platform, there exists a set of positive cable tensions such the moving-platform remains in static equilibrium. These poses can be computed from

$$\{\boldsymbol{X} | \boldsymbol{F}_o = \boldsymbol{A}\boldsymbol{\tau}, \boldsymbol{\tau} \geq \mathbf{0}\} \tag{8}$$

where $\boldsymbol{\tau}$ is the vector of the cable forces, $\boldsymbol{A} = -\boldsymbol{J}^T$ is the structure matrix of the robot and $\boldsymbol{F}_o$ is the external wrench applied to the end-effector. Analysis of the null space of the structure matrix is a common approach to determine WCW. Based on this approach the pose belongs to WCW when the Jacobian matrix of the robot is full rank and the null space of the structure matrix contains a vector $\boldsymbol{z} > \mathbf{0}$ ($\boldsymbol{A}\boldsymbol{z} = \mathbf{0}$).

According to this fact, one solution for (1) can be written as follows:

$$\boldsymbol{\tau} = \mathbf{A}^\dagger\mathbf{F}_o + \boldsymbol{Q} \tag{9}$$

where $\boldsymbol{A}^\dagger$ is the pseudo-inverse of the structure matrix and $\boldsymbol{Q}$ is the vector of internal forces among the cables. This term which lies in the null space of the structure matrix of the robot does not contribute to the movement of the end-effector and ensures us that all the cables are in tension. According to this fact, we should have

$$\boldsymbol{Q} = \tau_{max}\mathbf{N}_n \quad , \quad (\boldsymbol{A}\boldsymbol{N}_n = \mathbf{0} \ , \ \boldsymbol{N}_n > \mathbf{0}) \tag{10}$$

where τ_{max} is the norm of the internal forces and $\boldsymbol{N}_n$ is the normalized vector belongs to the null space of the structure matrix such that all its elements are positive. With this notation, it is clear that the internal force in each cable is less than τ_{max}. As it mentioned earlier, redundancy in actuation is necessary for the fully-constrained cable robots. For a robot with more than one degree of redundancy, $\boldsymbol{N}_n$ is a normalized linear combination of the null space vectors of the structure matrix such that all elements of $\boldsymbol{N}_n$ are positive. To find null space of the structure matrix for a mechanism with more than one degree of redundancy a method is presented in [12].

In some poses of the end-effector even in WCW, increasing τ_{max} may lead the robot to instability. In these poses, τ_{max} do

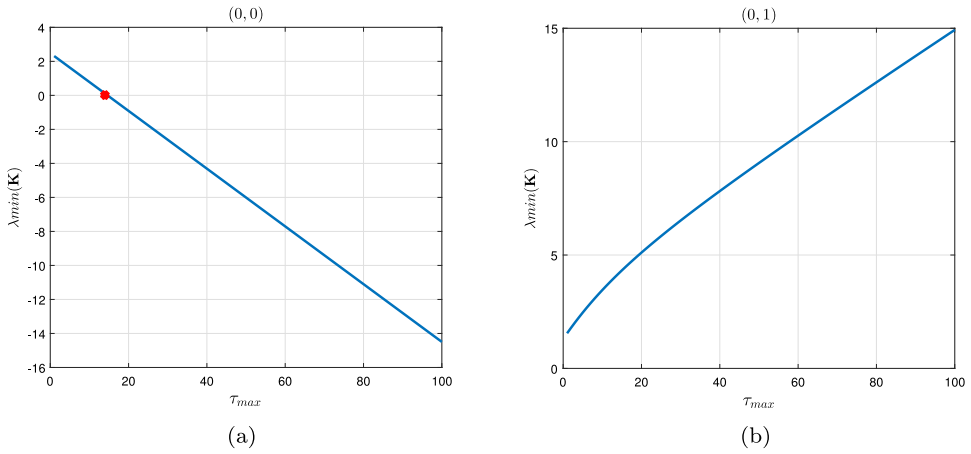

Fig. 3. Effects of the value of τ_{max} on the stability of the cable robot shown in Fig. 2.

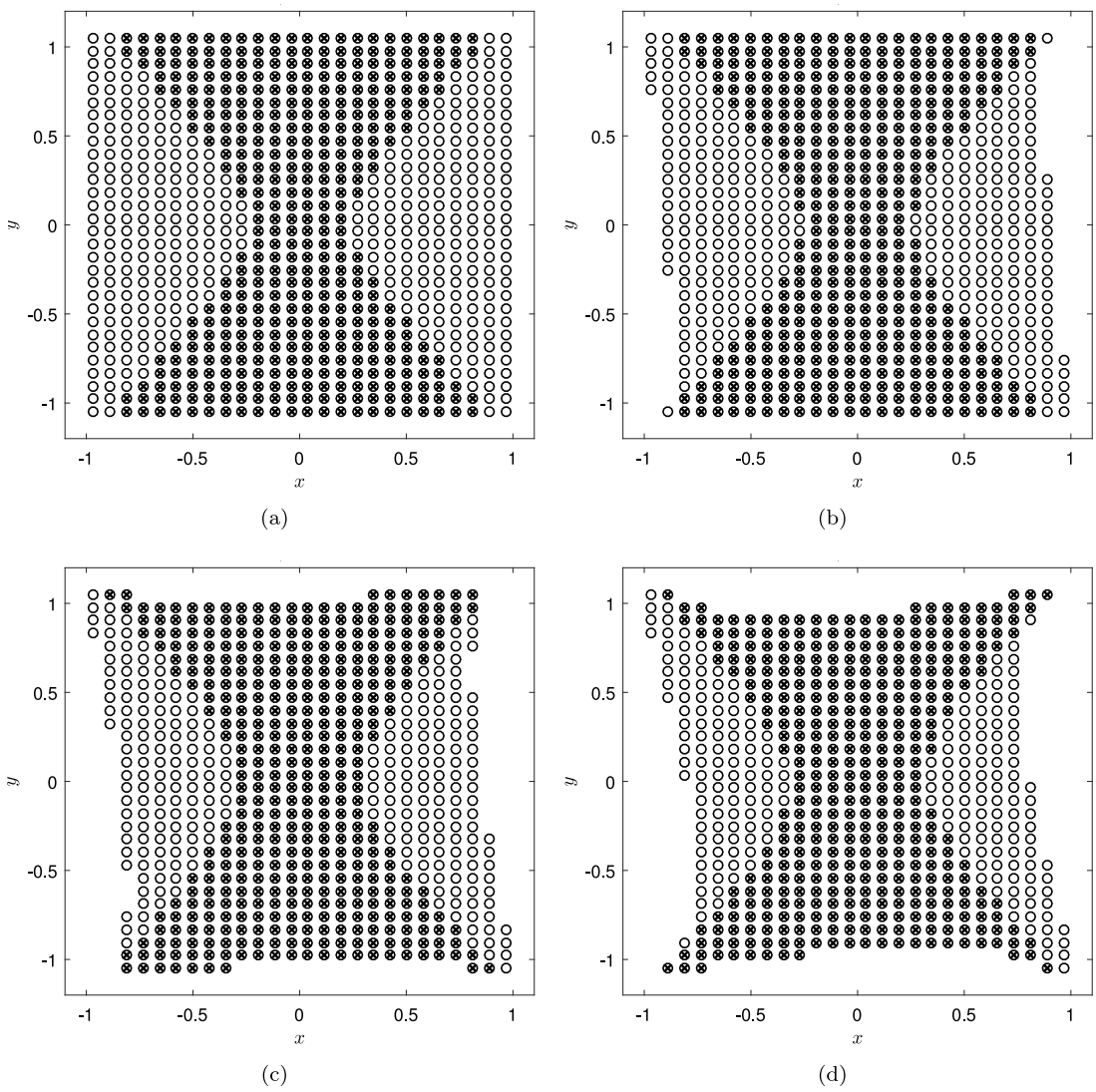

Fig. 4. The SFW (×) and WCW (◯) of a planar CDPR for τ_{max} up to 12N in four different orientation of the end-effector:(a) 0 deg, (b) 10 deg. (c) 20 deg, (d) 30 deg.

not improve the stiffness of the robot and even may make the stiffness matrix of the robot becomes negative. Whereas, in many applications, it is required that in the whole maneuver space of the robot, the end-effector works on some specific stiffness values and thus determining the stabilizable poses of the end-effector is essential. As it is known, the eigenvalues of the stiffness matrix present the stiffness of the manipulator in the direction of the corresponding eigenvectors. Thus, the minimum eigenvalue of the stiffness matrix in each pose of the end-effector can be employed as a criterion for determination of positive definiteness of the stiffness

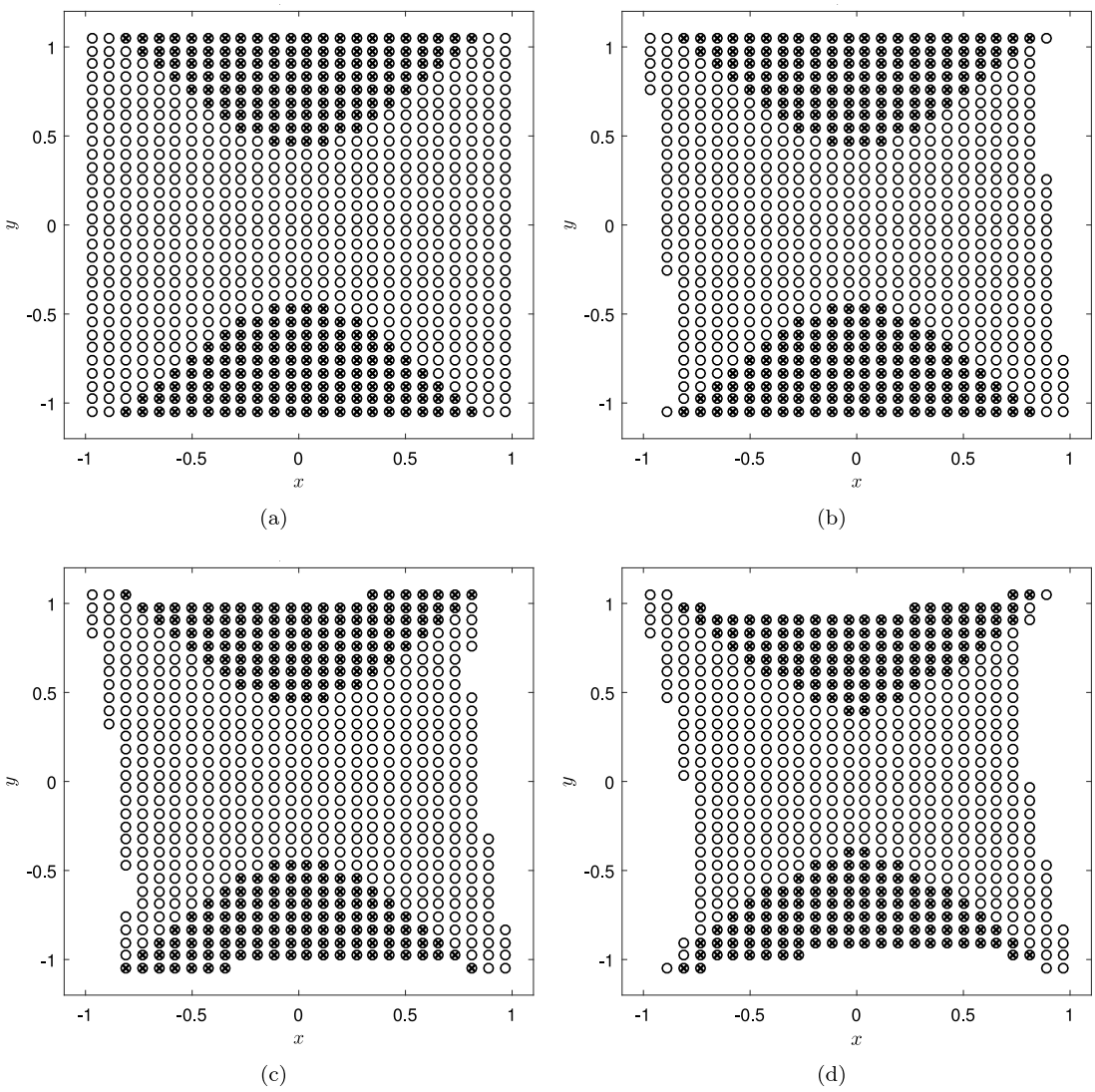

Fig. 5. The SFW (×) and WCW (◯) of a planar CDPR for τ_{max} up to 80N in four different orientation of the end-effector:(a) 0 deg, (b) 10 deg. (c) 20 deg, (d) 30 deg.

matrix or stabilizability of that pose and thus, it can describe the effects of τ_{max} on the stiffness of the robot.

For clarifying the effects of τ_{max} on stiffness and stability of CDPRs, a planar CDPR with three DOF is considered as the one shown in Fig. 2 and changes of τ_{max} on the minimum eigenvalue of the stiffness matrix is investigated as shown in Fig. 3. Two different positions (0,0) and (0,1) have been depicted in this figure. In Fig. 3(a) point (x=13.75,y=0) is a border between stability and instability of robot. Indeed, by increasing τ_{max} more than 13.75N, $\lambda_{min}(\mathbf{K})$ will be negative and the end-effector of robot becomes unstable. However, in Fig. 3(b) pose of the robot is stable for any value of the internal forces. Therefore, these conditions highly depend on the pose of end-effector and value of τ_{max}.

Based on the above-mentioned facts, defining an appropriate workspace that considers the stability of the robot and the internal forces limitations is essential. The most appropriate workspace to be proposed is the *Stiffness-Feasible Workspace*(SFW) and can be defined as follows:

Definition 1. The Stiffness-Feasible Workspace of a cable-driven parallel robot is a set of end-effector poses belong to Wrench Closure Workspace (WCW) of the robot in which for any value of the internal forces in the range of $(0\,,\ \tau_{max})$ total stiffness matrix of the robot is positive definite. (Minimum eigenvalue of the total stiffness matrix of the mechanism is positive.)

A pose of the end-effector belongs to the SFW is called a stiffness-feasible pose. With this definition, some properties of the SFW can be presented as follows:

Property 1. The SFW is a subset of WCW.
Property 2. SFW determines the allowable internal forces range $(0,\ \tau_{max})$ that guarantee the stability of the robot and tension-ability condition.
Property 3. The SFW of CDPR is the function of internal forces and the robot configuration such as the location of cables attachment points.

To clarify Definition 1, planar cable-driven parallel robot demonstrated in Fig. 2 is considered again, and stiffness-feasibility analysis of this robot is illustrated in Figs. 4 and 5. Both figures show the WCW and SFW of the robot for four constant orientations. In these figures circles and times show wrench closure workspace and stiffness-feasible workspace of CDPR, respectively. It is fascinating to note that some circles are not marked by times even for low values of τ_{max}. That means these poses are not stiffness feasible. Moreover, there are some poses that for any value of τ_{max} are not stiffness feasible. To point out the importance of this issue, another example is illustrated in Fig. 6. In this figure, the same CDPR with different configuration and the same value of τ_{max} is studied. It can be seen that in the whole WCW of the robot there is not any

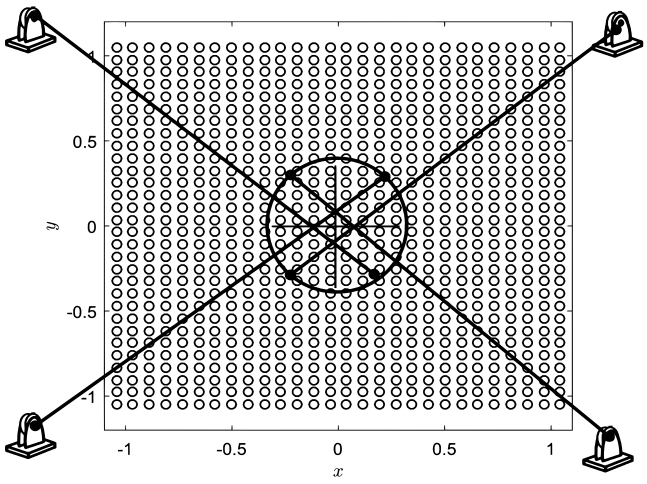

Fig. 6. Instability in everywhere of the WCW (SFW (×) and WCW (◯)).

stiffness-feasible pose. As a result, in each pose of the end-effector, stiffness-feasibility of CDPR depends on robot configuration and values of τ_{max}.

Limitation of CDPRs such as unstable poses and negative effects of the internal forces are mentioned in this section. Therefore, to reduce the mentioned limits of CDPRs, it is aimed to find optimal design. To achieve this goal, novel criteria are proposed in the next section.

4. Optimization criteria

One of the most important challenges in design and position control of the robot is to avoid singular poses. There are three common singularities which may occur in CDPRs [28]. One of them occurs when the Jacobian matrix has a rank deficiency or there are not internal forces at that pose. Thus, to avoid this type of singularity, the end-effector of CDPRs should always be in WCW. Furthermore, because of the unavoidable destructive effects of the internal forces in CDPRs, it is desired that the pose of the end-effector be located in SFW. In the following subsections, some criteria for the optimal design of CDPRs are defined based on the stiffness-feasible workspace.

4.0.1. Volume of the stiffness-feasible workspace

As it mentioned in Section 3, all parts of the WCW of the robot cannot be stiffness-feasible. Whereas, in the most of the applications, a mechanism with maximum stiffness-feasible workspace is valuable. Hence, the volume of SFW can be considered as a criterion for the optimal design of CDPRs to improve performance and low stiffness of these mechanisms. According to this necessity, in this paper maximizing the volume of the SFW and WCW are chosen as the objective functions.

4.0.2. Stiffness number

Eigenvalues of the stiffness matrix determine the stiffness of the end-effector in the direction of the corresponding eigenvectors. Thus, along different directions in the workspace of the robot, the stiffness of the end-effector may be different.[29]. However, in many applications, it is aspired to have uniform distribution stiffness in all directions. In this case, stiffness number of the stiffness matrix can be considered as a proper index. The stiffness number can be defined as the ratio of the minimum eigenvalue of the stiffness matrix over its maximum eigenvalue, as follows

$$SN = \frac{\lambda_{min}(\mathbf{K})}{\lambda_{max}(\mathbf{K})} \tag{11}$$

Based on the definition, in the stiffness-feasible workspace λ_{min} is positive and thus, in this workspace, the stiffness number is between 0 to 1. When the stiffness number is close to one, distribution of the stiffness of the mechanism at that pose will be uniform.

On the other hand, in order to deal with the non-homogeneity of the stiffness matrix terms, the stiffness matrix can be separated based on the method presented in [30]. As we know, one can write the following equation for the stiffness matrix

$$\mathbf{F}_o = \begin{bmatrix} \mathbf{K}_{11} & \mathbf{K}_{12} \\ \mathbf{K}_{21} & \mathbf{K}_{22} \end{bmatrix} \times \begin{bmatrix} \boldsymbol{\delta} \\ \boldsymbol{\omega} \end{bmatrix} \tag{12}$$

where $\boldsymbol{F}_o = [\boldsymbol{S}_i, \boldsymbol{M}_i]^T$ is vector of the external wrench, and δ and ω are infinitesimal translation and rotation of the end-effector, respectively. With this notation, unit-homogenized matrices, one for force and one for moment, can be present as follow,

$$\mathbf{U}_f = \begin{bmatrix} \boldsymbol{K_{11}O_{K_{11}}} & \boldsymbol{K_{12}O_{K_{12}}} \end{bmatrix} \tag{13}$$

$$\mathbf{U}_m = \begin{bmatrix} \boldsymbol{K_{21}O_{K_{21}}} & \boldsymbol{K_{22}O_{K_{22}}} \end{bmatrix} \tag{14}$$

in which $\mathbf{U}_f$ and $\mathbf{U}_m$ are stiffness unit-homogenized matrices corresponding to force and moment. Moreover, $\mathbf{O}_{K_{11}}$, $\mathbf{O}_{K_{12}}$, $\mathbf{O}_{K_{21}}$ and $\mathbf{O}_{K_{22}}$ are orthogonal matrices whose columns are the eigenvectors of matrices $\boldsymbol{K_{11}^T K_{11}}$, $\boldsymbol{K_{12}^T K_{12}}$, $\boldsymbol{K_{21}^T K_{21}}$ and $\boldsymbol{K_{22}^T K_{22}}$, respectively. By using eigenvalues of the unit-homogenized matrices $\boldsymbol{U}_f\boldsymbol{U}_f^T$ and $\boldsymbol{U}_m\boldsymbol{U}_m^T$, SN can be defined.

The Stiffness number is a local index and it is different in each pose of the end-effector. Therefore, in the whole SFW workspace, the global stiffness number index can be formulated as:

$$ASN = \frac{\int_g SN dg}{\int_g} \tag{15}$$

where g is the volume of stiffness-feasible workspace and SN is the stiffness number. ASN indicates how far the robot is from the uniform distribution stiffness. Larger ASN is desirable for performance and stiffness of the robot. Hence, the average of SN is selected as a criterion for the optimal design of CDPRs and the objective of optimization is to maximize the average of SN.

It should be mentioned that the criteria and definition presented in the previous sections can easily be extended and apply to cable robots driven with more than four cables and the spatial CDPRs. Because of access to geometrical and mechanical parameters of the NASIR and reduce computation, without loss of generality, in the following section we restrict ourselves to the planar cable robots.

5. Design parameters

In this section to define an optimal design formulation and reducing the number of design parameters, an initial design configuration with respect to the volume of SFW and WCW is introduced. The volume of SFW is obtained from poses under the condition of Definition 1 which depends on the configuration of the robot.

Initial design configuration of planar CDPR is illustrated in Fig. 7, where θ_B is the location of cable attachment points on the end-effector plane and R_B is the radius of the end-effector. In this figure, actuators positions are determined by A_i.

Without loss of generality, to reduce the computations of the optimization, the attachment points of cables on the end-effector plane are considered symmetric with respect to the x, y axes. Thus, by specifying the position of one of the cables, the other cables can be arranged to the end-effector plane in a rectangular pattern. Therefore, the position of the attachment points is always in a circle with a radius of R_B. These attachment points are defined as follows:

$$\theta_{B_4} = \theta_B\ ,\ \theta_{B_3} = \pi - \theta_{B_4}\ ,\ \theta_{B_1} = -\theta_{B_3}\ ,\ \theta_{B_2} = -\theta_{B_4} \tag{16}$$

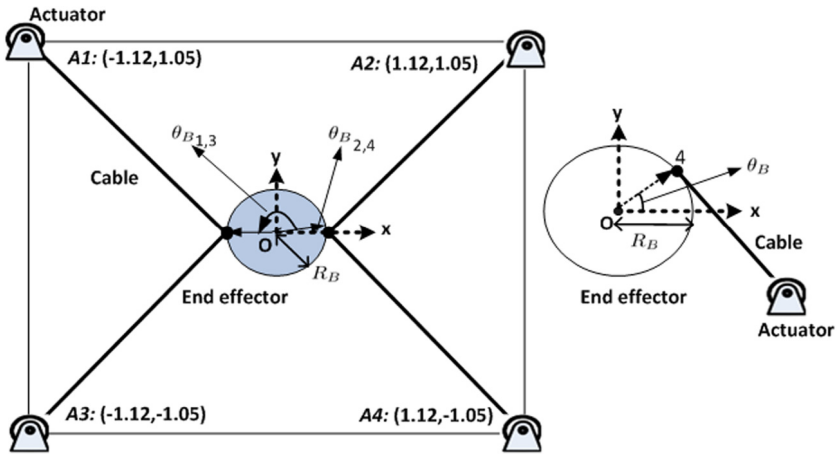

Fig. 7. Configuration of planar cable-driven parallel robots.

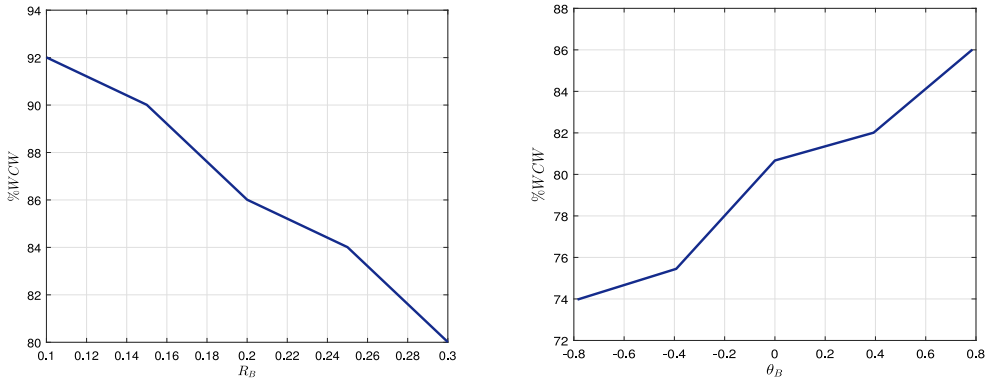

Fig. 8. Effects of design parameters R_B and θ_B on WCW.

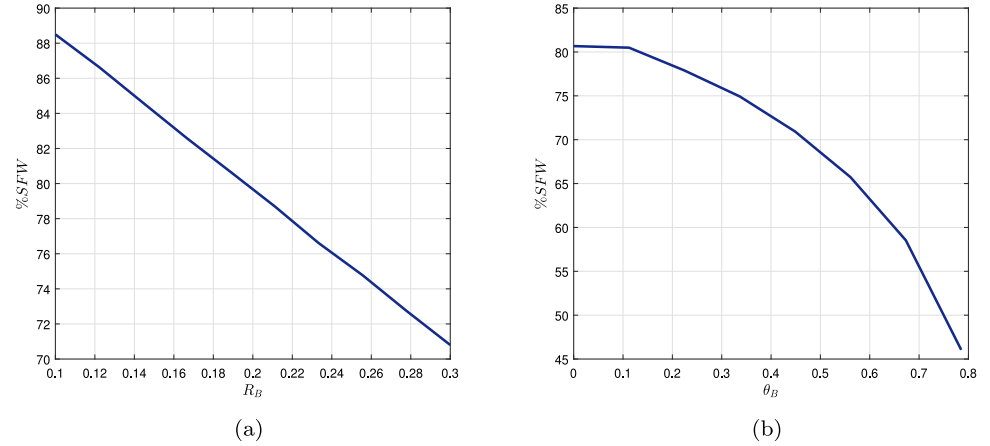

Fig. 9. Effects of design parameters R_B and θ_B on SFW.

In order to attach the cables in crossed form, the design parameter constraints are defined as follows:

$$0 \leq \theta_B \leq \pi/4\,,\ 0.1 \leq R_B \leq 0.3 \tag{17}$$

To investigate the relations between the design parameters and the proposed criteria, the robot shown in Fig. 7 is considered and the effects of design parameters (17) on percent of SFW, WCW, and average of SN are obtained and shown in Figs. 8–10. To have a better judgment about the effects of design parameters on the proposed criteria, the value of τ_{max} is selected 80N in all figures.

It has been illustrated in Fig. 8(a) that by increasing R_B the percentage of the WCW is decreased. While, the results in Fig. 8(b) confirm that by increasing θ_B the volume of WCW is increased. Figs. 9(a) and 9(b) illustrate that percentage of SFW is decreased by increasing θ_B and R_B. Furthermore, in Fig. 10 it has been shown that by increasing R_B average of stiffness number is increased and by increasing θ_B, the average of stiffness number is decreased. Therefore, the effects of design parameter R_B on SFW and WCW and the effect of design parameter θ_B on SFW and average of SN are similar.

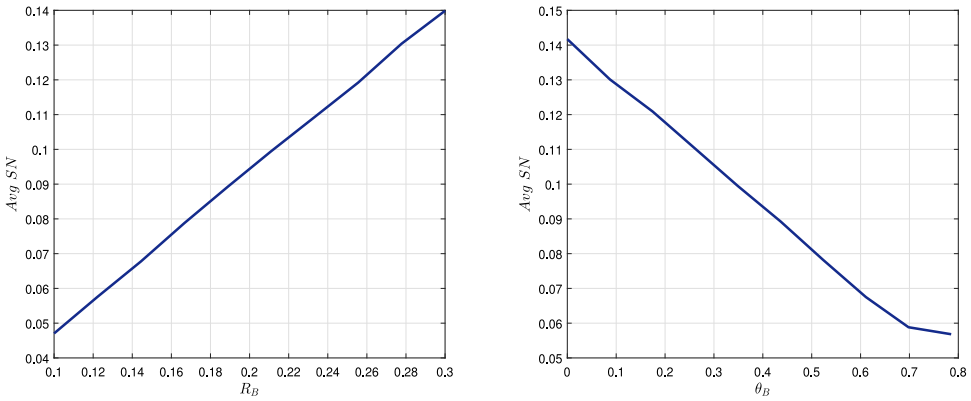

Fig. 10. Effects of design parameters R_B and θ_B on average of SN.

Table 1
Technical specifications of NASIR cable-driven parallel robot.

Specification	Value
Degree of freedom	3
Search space ($Length \times width$)	2.24×2.10 (m)
Available rotation	30 (Degree)

Table 3
NSGA-II parameters.

Parameter	Value
Population size	100
Number of generations	100
Crossover probability	0.8
Mutation probability	0.3

Table 2
Position of actuators on fixed frame.

Position of actuators	
$A_1(-1.12,1.05)$, $A_2(1.12,1.05)$	$A_3(-1.12,-1.05)$, $A_4(1.12,-1.05)$

Based on this investigation, it should be noted that there is a contradiction between increasing θ_B in SFW with WCW as well as a contradiction between increasing R_B in SFW and WCW with the average of SN. Therefore, these conflicts between optimization criteria motivate us to use multi-objective methods.

6. Optimal design of planar cable-driven parallel robot

For optimal design, a planar CDPR with three DOF and four actuators is considered in which cables are connected to the end-effector plane in different attachment points. The position of the attachment points can be varied to show the effects of attachment points on the proposed criteria. Technical specifications of this robot and location of the actuators, which are similar to NASIR planar cable-driven parallel robot are selected as Tables 1 and 2, respectively [31].

The percentage of SFW and WCW respect to the search space defined in Table 2 are introduced as criteria and the objective function is to maximize the percentage of WCW and SFW. In order to determine the WCW and SFW, a mesh on the search space of the robot is taken and the percentage of the WCW and SFW is determined. The dimension of the robot is illustrated at Table 2, the distance between this dimension divided into 100×100 points. Stiffness-feasibility and the wrench-closure ability of the end-effector of the robot in each point are investigated by Definition 1 and elements of the null space of the structure matrix, respectively. Finally, these criteria are presented as the percentage of the whole investigated space.

Based on the contradiction between design criteria, the NSGAII algorithm in MATLAB is initialized by using parameters that are shown in Table 3 and $\tau_{max} = 80N$. The optimization converges to the optimal cable configuration, where WCW and SFW are maximized. Contradiction between the proposed criteria leads the optimization algorithm to a Pareto front. Results of the Pareto front are listed on Table 4.

It is interesting to note that considering the volume of WCW, the case 4 is the best. Whereas, this case provides poor behavior as far as the volume of SFW is the concern. On the other hand, it was shown in Fig. 8 and Fig. 9 that by increasing R_B, WCW and SFW will be decreased. Therefore, in Table 4, R_B for all cases is obtained 0.1.

In order to select the best answer from the Pareto front, answers are constrained as follows:

$$\%WCW \geq 70\ ,\ \%SFW \geq 50 \tag{18}$$

By considering all of these constraints, case 3 and case 5 are the best answers. However, θ_B in case 3 is more than case 5 and thus, the 3rd case leads the end-effector to have more orientation on the workspace. Hence, in the application requiring more orientation case 3 is proper. According to this fact, optimal parameters for planar CDPR are determined as follows:

$$\begin{aligned} &\theta_{B_4} = 37.71^\circ\ ,\ \theta_{B_3} = 142.29^\circ\ ,\ \theta_{B_2} = -37.71^\circ, \\ &\theta_{B_1} = -142.29^\circ\ ,\ R_B = 0.1(m) \end{aligned} \tag{19}$$

6.0.1. Weighted optimization

In order to optimally design of CDPRs, in addition to maximized SFW and WCW and for achieving uniform distribution stiffness, a weighted optimization approach is defined. Therefore, a multi-objective problem is transformed into a single objective problem. In this approach integrated optimization goal is expressed as follows:

$$\begin{aligned} &\min \sum_{k=1}^{n_k} w_k f_k(x) \\ &w_k \geq 0\ \ k = 1, \ldots, n_k \end{aligned} \tag{20}$$

where w_k is weight of criteria, k and f_k are number of the optimization criteria and the objective function, respectively. Weights of criteria will be chosen according to the importance of each criterion. Hence, optimization function is defined as follows:

$$f(x_i) = w_1 f1(x_i) + w_2 f2(x_i) + w_3 f3(x_i) \tag{21}$$

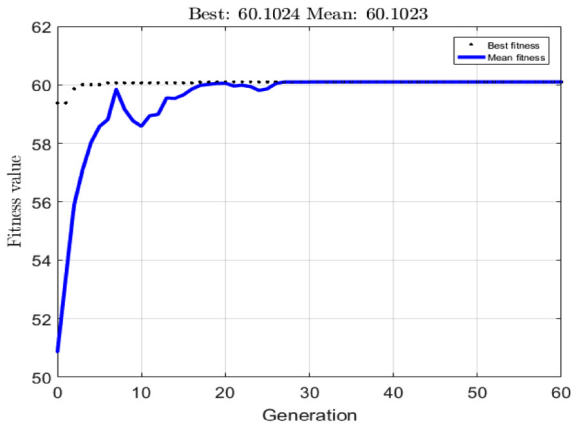

Fig. 11. Convergence of the GA procedure.

Table 4
Optimal results of planar CDPR.

	%WCW	%SFW	θ_B	R_B
1	68	62.05	25.25	0.1
2	66	64.53	16.44	0.1
3	72	53.13	37.71	0.1
4	74	45.45	42.71	0.1
5	70	58.65	31.97	0.1

where $i = 1, \ldots, 3$, f1, f2 and f3 are WCW, SFW and the average of SN, respectively. w_i are weight of each optimization criteria. Let us define the weights as follows:

$$w_1 = w_2 = 1/3, w_3 = 100/3 \tag{22}$$

According to this fitness function, a planar CDPR is designed with Genetic Algorithm setup same as given in Table 3 and τ_{max} is equal to 80N. Results of this optimization is illustrated in Fig. 11. In this figure, the convergence of the GA algorithm is shown. It can be seen that GA algorithm converges to 60.1024 and optimal parameters for a planar CDPR is obtained as follows:

$$\theta_{B_4} = 0^\circ\ ,\ \theta_{B_3} = 180^\circ\ ,\ \theta_{B_2} = 0^\circ\ ,\ \theta_{B_1} = 180^\circ\ ,\ R_B = 0.1(m) \tag{23}$$

To have a better judgment about the obtained optimal parameters, consider NASIR cable-driven robot (Fig. 12) [32]. The design parameters of this robot such as the position of attachment points and the radius of the end-effector are shown in this figure and given in Tables 1 and 2. Four moving attachment points of this planar cable-driven robot firstly were attached to the end-effector in cross cable form to achieve maximum wrench closure workspace. According to the adverse effects of the internal forces on the stiffness matrix, the robot was collapsed and an unprecedented movement happened at the end-effector. Therefore, based on the experimental results, another configuration was selected for the robot as shown in Fig. 12 and it is interesting that the selected parameters match optimal design parameters given in (23).

7. Conclusion

In this paper, relying on the essential role of the internal forces in operation of the cable-driven parallel robots, a novel stiffness-feasible workspace based on the internal forces stiffness and their effects on the performance of the CDPRs is proposed. This type of workspace is the outcome of the analysis of the wrench closure workspace and the stiffness matrix of the robot. In this workspace, the allowable internal forces range in order to increase the stiffness is specified which will guarantee that in this range of internal forces, the end-effector of the robot is stiffness-feasible. Furthermore, considering the stability of the end-effector of the robot, another criterion which is useful to analyze the uniform distribution of stiffness is introduced. Due to the contradictory effects of design parameters on the volume of the stiffness-feasible workspace, the volume of the wrench closure workspace, and the average of stiffness number, a multi-objective optimization is provided. Simulation results are presented to confirm the effectiveness of the proposed optimization.

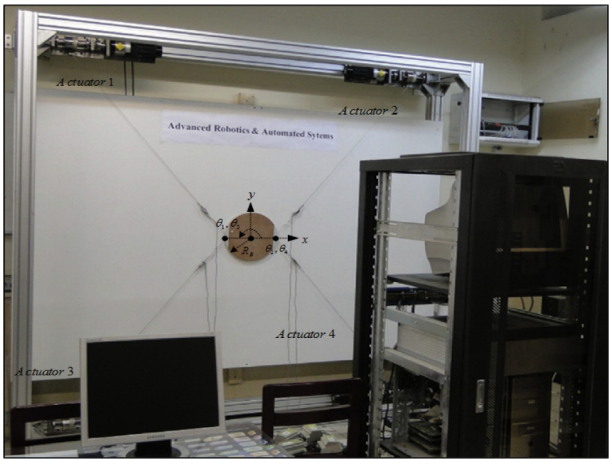

Fig. 12. Prototype of NASIR planar cable driven robot.

References

[1] M.A. Khosravi, H.D. Taghirad, Dynamic analysis and control of cable driven robots with elastic cables, Trans. Can. Soc. Mech. Eng. 35 (4) (2011) 543–558.
[2] S. Qian, B. Zi, W.-W. Shang, Q.-S. Xu, A review on cable-driven parallel robots, Chin. J. Mech. Eng. 31 (1) (2018) 66.
[3] M.H. Korayem, H. Tourajizadeh, Maximum DLCC of spatial cable robot for a predefined trajectory within the workspace using closed loop optimal control approach, J. Intell. Robot. Syst. 63 (1) (2011) 75–99.
[4] L.L. Cone, SKYCAM-An aerial robotic camera system, Byte 10 (10) (1985) 122.
[5] D. Chakarov, Study of the antagonistic stiffness of parallel manipulators with actuation redundancy, Mech. Mach. Theory 39 (6) (2004) 583–601.
[6] M. Nahon, G. Gilardi, C. Lambert, Dynamics/control of a radio telescope receiver supported by a tethered aerostat, J. Guid. Control Dyn. 25 (6) (2002) 1107–1115, http://dx.doi.org/10.2514/2.4990.
[7] P.D. Campbell, P.L. Swaim, C.J. Thompson, Charlotte robot technology for space and terrestrial applications, 1995, http://dx.doi.org/10.4271/951520,
[8] R.G. Roberts, T. Graham, T. Lippitt, On the inverse kinematics, statics, and fault tolerance of cable-suspended robots, J. Field Robot. 15 (10) (1998) 581–597, http://dx.doi.org/10.1002/(SICI)1097-4563(199810)15:10<581::AID-ROB4>3.0.CO;2-P.
[9] M.H. Korayem, M. Bamdad, H. Tourajizadeh, A.H. Korayem, S. Bayat, Analytical design of optimal trajectory with dynamic load-carrying capacity for cable-suspended manipulator, Int. J. Adv. Manuf. Technol. 60 (1–4) (2012) 317–327.
[10] M.A. Khosravi, H.D. Taghirad, Experimental performance of robust pid controller on a planar cable robot, in: Cable-Driven Parallel Robots, Springer, 2013, pp. 337–352.
[11] M. Gouttefarde, C.M. Gosselin, Analysis of the wrench-closure workspace of planar parallel cable-driven mechanisms, IEEE Trans. Robot. 22 (3) (2006) 434–445.
[12] A.Z. Loloei, H.D. Taghirad, Controllable workspace of cable-driven redundant parallel manipulators by fundamental wrench analysis, Trans. Can. Soc. Mech. Eng. 36 (3) (2012) 297–313.
[13] J. Pusey, A. Fattah, S. Agrawal, E. Messina, Design and workspace analysis of a 6–6 cable-suspended parallel robot, Mech. Mach. Theory 39 (7) (2004) 761–778.
[14] B. Ouyang, W. Shang, Wrench-feasible workspace based optimization of the fixed and moving platforms for cable-driven parallel manipulators, Robot. Comput.-Integr. Manuf. 30 (6) (2014) 629–635.
[15] M. Horoub, M. Hawwa, Influence of cables layout on the dynamic workspace of a six-dof parallel marine manipulator, Mech. Mach. Theory 129 (2018) 191–201.

[16] B. Zhang, W.W. Shang, S. Cong, Y. Liu, Size optimization of the moving platform for cable-driven parallel manipulators based on stiffness characteristics, Proc. Inst. Mech. Eng. Pt. C J. Mech. Eng. Sci. 232 (11) (2018) 2057–2066.
[17] S. Kawamura, H. Kino, C. Won, High-speed manipulation by using parallel wire-driven robots, Robotica 18 (1) (2000) 13–21, http://dx.doi.org/10.1017/S0263574799002477.
[18] S. Yeo, G. Yang, W. Lim, Design and analysis of cable-driven manipulators with variable stiffness, Mech. Mach. Theory 69 (2013) 230–244.
[19] H. Yuan, E. Courteille, D. Deblaise, Static and dynamic stiffness analyses of cable-driven parallel robots with non-negligible cable mass and elasticity, Mech. Mach. Theory 85 (2015) 64–81, http://dx.doi.org/10.1016/j.mechmachtheory.2014.10.010.
[20] S. Behzadipour, A. Khajepour, Stiffness of cable-based parallel manipulators with application to stability analysis, J. Mech. Design 128 (1) (2006) 303–310.
[21] S. Abdolshah, D. Zanotto, G. Rosati, S.K. Agrawal, Optimizing stiffness and dexterity of planar adaptive cable-driven parallel robots, J. Mech. Robot. 9 (3) (2017) 031004, http://dx.doi.org/10.1115/1.4035681.
[22] J. Bolboli, M.A. Khosravi, F. Abdollahi, Analysis of the stiffness feasible workspace of the cable-driven parallel robots, in: 2017 5th RSI International Conference on Robotics and Mechatronics (ICRoM), IEEE, 2017, pp. 45–50.
[23] X. Zhou, S.-k. Jun, V. Krovi, Stiffness modulation exploiting configuration redundancy in mobile cable robots, in: Robotics and Automation (ICRA), 2014 IEEE International Conference on, 2014, pp. 5934–5939. http://dx.doi.org/10.1109/ICRA.2014.6907733.
[24] K. Yu, L.-F. Lee, V.N. Krovi, Simultaneous trajectory tracking and stiffness control of cable actuated parallel manipulator, in: Int. Design Engineering Technical Conf. & Computers and Information in Engineering Conf, 2009. http://dx.doi.org/10.1115/DETC2009-87457.
[25] H. Jamshidifar, A. Khajepour, B. Fidan, M. Rushton, Kinematically-constrained redundant cable-driven parallel robots: modeling, redundancy analysis, and stiffness optimization, IEEE/ASME Trans. Mechatronics 22 (2) (2017) 921–930, http://dx.doi.org/10.1109/TMECH.2016.2639053.
[26] S. Torres-Mendez, A. Khajepour, Design optimization of a warehousing cable-based robot, in: Proc. 2014 ASME Int. Des. Eng. Tech. Conf. Comput. Info. Eng. Conf., 2014, pp. V05AT08A091–V05AT08A099, http://dx.doi.org/10.1115/DETC2014-34672.
[27] L. Notash, A. Moradi, Optimizing layout of a planar wire-actuated parallel manipulator based on stiffness and failure analyses, Trans. Can. Soc. Mech. Eng. 36 (2) (2012) 195–205.
[28] M. Gouttefarde, S. Krut, O. Company, F. Pierrot, N. Ramdani, On the design of fully constrained parallel cable-driven robots, Adv. Robot Kinemat. Anal. Des. (2008) 71–78, http://dx.doi.org/10.1007/978-1-4020-8600-7-8.
[29] A. Moradi, Stiffness analysis of cable-driven parallel robots, Queen's University, Canada, 2013.
[30] A. Taghaeipour, J. Angeles, L. Lessard, Online computation of the stiffness matrix in robotic structures using finite element analysis, in: Department of Mechanical Engineering and Centre for Intelligent Machines, McGill University, Montreal, 2010.
[31] M.A. Khosravi, H.D. Taghirad, Dynamic analysis and control of fully-constrained cable robots with elastic cables: variable stiffness formulation, in: Cable-Driven Parallel Robots, 2015, pp. 161–177, http://dx.doi.org/10.1007/978-3-319-09489-2-12.
[32] M.A. Khosravi, H.D. Taghirad, Dynamic modeling and control of parallel robots with elastic cables: singular perturbation approach, IEEE Trans. Robot. 30 (3) (2014) 694–704, http://dx.doi.org/10.1109/TRO.2014.2298057.

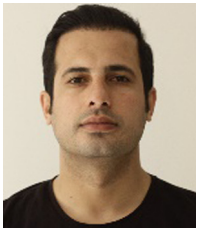

Javad Bolboli received the B.Sc. degree in electrical engineering from the Sadjad University of Technology, Mashhad, Iran, the M.Sc. degree in electrical engineering from the Amirkabir University of Technology, Tehran, Iran. His current research interests include robotics, optimization, control of nonlinear systems, Control of multi-agent networks, neural networks, and machine learning. He is affiliated with IEEE as student member.

Mohammad A. Khosravi received the M.Sc. degree from K. N. Toosi University of Technology, Tehran, Iran, in 2000, and the Ph.D. degree from K. N. Toosi university of Technology, Tehran, Iran in 2013, all in electrical engineering. He is currently an assistant professor with Amirkabir University of Technology. His research interests lie in the areas of parallel robotics, cable driven robots, robust control and nonlinear control theory.

Farzaneh Abdollahi received the B.Sc. degree in electrical engineering from Isfahan University of Technology, Isfahan, Iran, in 1999, the M.Sc. degree in electrical engineering from Amirkabir University of Technology, Tehran, Iran, in 2003, and the Ph.D. degree in electrical engineering from Concordia University, Montreal, C, Canada, in 2008. She is currently an Assistant Professor with Amirkabir University of Technology and a Research Assistant Professor with Concordia University. Her research interests include neural networks, robotics, control of nonlinear systems, control of multiagent networks, and robust and switching.